
Extended Meshfree Method for Elastic and Inelastic Media

Jiun-Shyan Chen¹ and Dongdong Wang²

¹ Department of Civil and Environmental Engineering, University of California, Los Angeles, CA 90095-1593, USA jschen@seas.ucla.edu

² Department of Civil and Environmental Engineering, University of California, Los Angeles, CA 90095-1593, USA ddwang@seas.ucla.edu

Abstract

In this paper, an extended meshfree method [9] for solving elastic boundary value problems is summarized, and its extension to the elasto-plasticity problem is presented. In extended meshfree method, the solution is decomposed into particular solution and homogeneous solution. The particular solution without satisfying boundary conditions is obtained analytically, while a homogeneous problem with auxiliary boundary conditions is then solved under a Galerkin framework with moving least-squares reproducing kernel approximation. The proposed method for linear differential operator in Poisson, elasticity, and Mindlin-Reissner problems is first summarized. The extension to differential equations with nonlinear self-adjoint differential operator is then introduced, and the application to elasto-plasticity problem is presented. Numerical results of an elasto-plasticity problem demonstrate a significant accuracy gain in the solution of extended meshfree method compared to that of the conventional Galerkin meshfree approach.

1 Introduction

The naturally conforming properties of Galerkin meshfree methods offer tremendous flexibility for approximation of solution with arbitrary locality and smoothness [1, 4, 6, 11, 18, 19]. For example, extended finite element method with enriched local basis functions was used to model crack tip characteristics [3, 10]. Hierarchical enrichment [16, 17, 22], coupling between FEM and meshfree methods [13, 15, 17], and interface enrichment [14, 24] were also developed for enhancement of local solutions. Partition of unity and generalized finite element method [1, 2, 11, 12, 19, 20, 21] provide a general framework for enrichment of solution with special basis functions to simultaneously achieve local and global solution accuracy.

Alternative to the aforementioned methods where the degrees of freedom associated with the global and enriched solutions are obtained concurrently, an extended meshfree method [9] has been proposed in which the solution is solved in 2 sequential steps. In this approach, the solution is decomposed into particular solution and homogeneous solution. The particular solution is solved by satisfying the differential equation containing the source term in an infinite domain without the imposition of boundary conditions. This particular solution can often be obtained analytically. When such particular solution in an infinite domain is available, the original problem can be reduced to a homogeneous problem with auxiliary boundary conditions (corrected by the particular solution) that is then solved numerically. It has been shown that if a linearly complete approximation function in conjunction with a stabilized conforming nodal integration for domain integration of the weak form are employed in the Galerkin approximation of PDE's, linear exactness and bending exactness [7, 8, 23] can be achieved in the numerical solution of potential and plate problems, respectively. These properties are particularly useful for solving homogeneous solution in solid and structural problems, where substantially higher solution accuracy can be obtained compared to the conventional Galerkin meshfree formulation.

In this paper, we first review the basic concept and solution procedures of extended meshfree method in Section 2. In this section, a general and straightforward approach is presented for constructing the particular solution by employing a fundamental solution of the differential operator without satisfying the boundary conditions. Consequently, only a homogeneous governing equation with auxiliary boundary conditions is solved by a Galerkin meshfree method with stabilized conforming nodal integration. The specific extended meshfree formulations for problems with linear differential operator such as Poisson, elasticity, and Mindlin-Reissner problems are discussed in Section 3. In section 4, we first discuss extended meshfree method for PDE's with non-linear self-adjoint differential operator. The application to elasto-plasticity problem and some comments on numerical procedures are then presented. Several numerical examples are demonstrated in Sections 3 and 4. Concluding remarks are given in Section 5.

2 Review of Extended Meshfree Method

2.1 Moving Least-Square Reproducing Kernel (MLS/RK) Approximation

The MLS/RK approximation [18] has been widely used in the meshfree approximation of the unknown variables in differential equations. The problem domain Ω is first discretized into a set of points $\{\mathbf{x}_1, \mathbf{x}_2, \dots, \mathbf{x}_{NP}\}$, where \mathbf{x}_I is the location of node I and NP denotes the total number of points. The unknown variable $u(\mathbf{x})$ of a differential equation is approximated by:

$$u^h(\mathbf{x}) = \sum_{I=1}^{NP} \Psi_I(\mathbf{x}) d_I \quad (1)$$

where $u^h(\mathbf{x})$ is the approximation of $u(\mathbf{x})$, Ψ_I and d_I are the shape functions and their associated coefficients, respectively. In MLS/RK approximation [18], a shape function $\Psi_I(\mathbf{x})$ takes the form:

$$\Psi_I(\mathbf{x}) = \left(\sum_{i+j=0}^n (x_1 - x_{1I})^i (x_2 - x_{2I})^j \bar{b}_{ij}(x) \right) \phi_a(\mathbf{x} - \mathbf{x}_I) \quad (2)$$

where $\phi_a(\mathbf{x} - \mathbf{x}_I)$ is a kernel function that defines the smoothness and locality of the approximation with a compact support $\omega_I = \text{supp}(\phi_a(\mathbf{x} - \mathbf{x}_I))$, where a is the radius of ω_I , and $\cup_{I=1}^{NP} \omega_I \supset \Omega$. The coefficient vector $\mathbf{b}(\mathbf{x})$ in Eq. (2) is obtained by satisfying the following n -th order reproducing conditions:

$$\sum_{I=1}^{NP} \Psi_I(\mathbf{x}) x_{I1}^\alpha x_{I2}^\beta = x_1^\alpha x_2^\beta, \quad \alpha + \beta = 0, 1, 2, \dots, n \quad (3)$$

Upon solving $\bar{b}_{ij}(x)$ from Eq. (3), the MLS/RK shape functions is obtained:

$$\Psi_I(\mathbf{x}) = \{\mathbf{H}\}^T(\mathbf{0}) \{\mathbf{M}\}^{-1}(\mathbf{x}) \{\mathbf{H}\}(\mathbf{x} - \mathbf{x}_I) \phi_a(\mathbf{x} - \mathbf{x}_I) \quad (4)$$

where

$$\{\mathbf{H}\}^T(\mathbf{x} - \mathbf{x}_I) = \{1, x_1 - x_{1I}, x_2 - x_{2I}, (x_1 - x_{1I})^2, \dots, (x_2 - x_{2I})^n\} \quad (5)$$

$$\{\mathbf{M}\}(\mathbf{x}) = \sum_{I=1}^{NP} \{\mathbf{H}\}(\mathbf{x} - \mathbf{x}_I) \{\mathbf{H}\}^T(\mathbf{x} - \mathbf{x}_I) \phi_{a_I}(\mathbf{x} - \mathbf{x}_I) \quad (6)$$

The reproducing kernel particle method (RKPM) is formulated by introducing the above approximation of unknown into the weak form of the differential equation $\mathcal{L}(u) + b = 0$ where \mathcal{L} is the differential operator and b is the source term. The order of the solution is mainly dependent upon the form of source term and the differential operator. The following problem introduced in [9] is solved to illustrate the property of the RKPM using a stabilized conforming nodal integration for domain integration [7], denoted as SC-RKPM, in representing the behavior of a localized high-gradient source term.

$$\begin{aligned} u_{,xx} + b(x) &= 0 \text{ in } (0, 1) \\ b(x) &= \begin{cases} \{2/\alpha^2 - 4[(x - 0.5)/\alpha]^2\} \exp\{ -[(x - 0.5)/\alpha]^2 \} & \text{for } 0.42 \leq x \leq 0.58 \\ 0 & \text{otherwise} \end{cases} \\ u(0) &= 0, \quad u(1) = 1 \end{aligned} \quad (7)$$

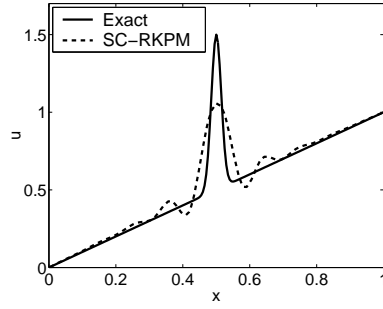


Fig. 1. Solution comparison for problem (7)

A comparison of the SC-RKPM solution using linear basis function with a 20-node discretization and exact solutions in Fig. 1 shows large differences in the vicinity of the localized source term. Figures 2 (a) and (b) demonstrate the effects of discretization with nodal distance ($h = 0.0625, 0.0313, 0.0156$) and the source term localization ($\alpha = 0.5, 0.3, 0.1$) on the error of solution accuracy using SC-RKPM. The results show that the L_2 error norm of u increases as the source term becomes more localized in all three discretizations. It is also shown that the level of localization α in the source term affects the constant of error in the numerical solution.

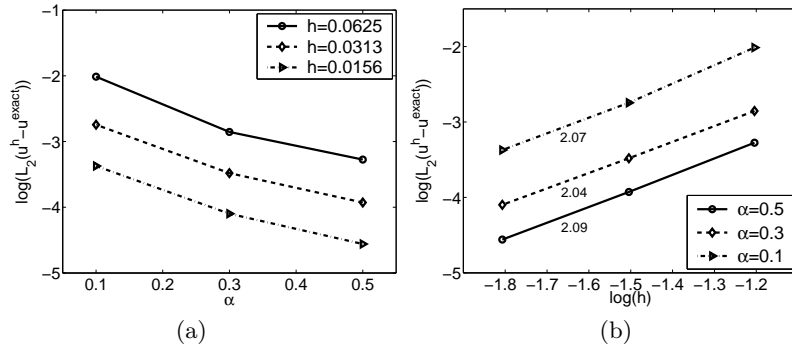


Fig. 2. Effects of discretization and source term localization on L_2 error norm of u in problem (7) using SC-RKPM

2.2 Extended Meshfree Method for Boundary Value Problems with Linear Differential Operator

Consider the following multi-dimensional boundary value problem (BVP):

$$\begin{aligned}\mathcal{L}(\mathbf{u}(\mathbf{x})) + \mathbf{b}(\mathbf{x}) &= \mathbf{0} \text{ in } \Omega \\ B_u(\mathbf{u}(\mathbf{x})) &= \mathbf{0} \text{ on } \partial_u \Omega \\ B_h(\mathbf{u}(\mathbf{x})) &= \mathbf{0} \text{ on } \partial_h \Omega\end{aligned}\quad (8)$$

where \mathcal{L} is the linear differential tensor operator, $\mathbf{b}(\mathbf{x})$ is the source term tensor, B_u and B_h are the tensor operators of essential and natural boundary conditions, respectively. Let $\mathbf{g}(\mathbf{x}, \bar{\mathbf{x}})$ be the fundamental solution tensor that satisfies the PDE in an *infinite domain* (i.e., without considering boundary conditions):

$$\mathcal{L}(\mathbf{g}(\mathbf{x}, \bar{\mathbf{x}})) + \delta(\mathbf{x} - \bar{\mathbf{x}}) = 0 \text{ in } \mathbb{R}^3 \quad (9)$$

or in a matrix form

$$[\mathbf{L}] \begin{Bmatrix} g_{11} \\ g_{21} \\ g_{31} \end{Bmatrix} + \begin{Bmatrix} \delta \\ 0 \\ 0 \end{Bmatrix} = \mathbf{0}, \quad [\mathbf{L}] \begin{Bmatrix} g_{12} \\ g_{22} \\ g_{32} \end{Bmatrix} + \begin{Bmatrix} 0 \\ \delta \\ 0 \end{Bmatrix} = \mathbf{0}, \quad [\mathbf{L}] \begin{Bmatrix} g_{13} \\ g_{23} \\ g_{33} \end{Bmatrix} + \begin{Bmatrix} 0 \\ 0 \\ \delta \end{Bmatrix} = \mathbf{0} \quad (10)$$

where $\delta = \delta(\mathbf{x} - \bar{\mathbf{x}})$, $[\mathbf{L}]$ is the 3×3 matrix corresponding to matrix expression of $\mathcal{L}(\mathbf{g}(\mathbf{x}, \bar{\mathbf{x}}))$, and $\delta(\mathbf{x} - \bar{\mathbf{x}})$ is the delta function. Then a particular solution is obtained by the integral:

$$\mathbf{u}^p(\mathbf{x}) = \int_{\Omega} \mathbf{g}(\mathbf{x}, \mathbf{y}) \cdot \mathbf{b}(\mathbf{y}) d\mathbf{y} \quad (11)$$

where “ \cdot ” is a inner product. From Eqns. (9) and (11), it can be easily shown that the particular solution \mathbf{u}^p satisfies

$$\mathcal{L}(\mathbf{u}^p(\mathbf{x})) + \mathbf{b}(\mathbf{x}) = \mathbf{0} \text{ in } \Omega \quad (12)$$

Note that in general $\mathbf{u}^p(\mathbf{x})$ does not satisfy boundary conditions, i.e., $B_u(\mathbf{u}^p(\mathbf{x})) \neq \mathbf{0}$, $B_h(\mathbf{u}^p(\mathbf{x})) \neq \mathbf{0}$. The expressions of fundamental solutions and particular solutions for Poisson equation, elasticity, and Mindlin-Reissner plate problems are listed in Table 1. Next, the solution of the given problem is decomposed into

$$\mathbf{u}(\mathbf{x}) = \mathbf{u}^p(\mathbf{x}) + \mathbf{u}^0(\mathbf{x}) \quad (13)$$

If \mathcal{L} is the linear differential operator, we have the following condition:

$$\mathcal{L}(\mathbf{u}(\mathbf{x})) + \mathbf{b}(\mathbf{x}) = \mathcal{L}(\mathbf{u}^p(\mathbf{x})) + \mathcal{L}(\mathbf{u}^0(\mathbf{x})) + \mathbf{b}(\mathbf{x}) = \mathcal{L}(\mathbf{u}^0(\mathbf{x})) = \mathbf{0} \quad (14)$$

This leads to the following BVP for the homogeneous solution $\mathbf{u}^0(\mathbf{x})$ (assuming B_u and B_h are linear operators):

$$\begin{aligned}\mathcal{L}(\mathbf{u}^0(\mathbf{x})) &= \mathbf{0} \text{ in } \Omega \\ B_u(\mathbf{u}^0(\mathbf{x})) &= -B_u(\mathbf{u}^p(\mathbf{x})) \text{ on } \partial_u \Omega \\ B_h(\mathbf{u}^0(\mathbf{x})) &= -B_h(\mathbf{u}^p(\mathbf{x})) \text{ on } \partial_h \Omega\end{aligned}\quad (15)$$

Here the homogeneous solution $\mathbf{u}^0(\mathbf{x})$ is obtained from the above homogeneous equation with boundary conditions modified by $\mathbf{u}^p(\mathbf{x})$. A few examples of fundamental solutions [5, 25] for linear differential operator are given in Table 1.

Table 1. Particular Solutions of Several Boundary Value Problems

	Poisson Equation	Elasticity	Mindlin-Reissner Plate
Tensor Form $\mathcal{L}(\mathbf{u}) + \mathbf{b} = \mathbf{0}$	$\nabla^2 u + b = 0$	$\nabla \cdot (\mathbf{C} : \nabla^s \mathbf{u}) + \mathbf{b} = \mathbf{0}$ $(\nabla^s \mathbf{u}) = (\nabla \otimes \mathbf{u} + \mathbf{u} \otimes \nabla) / 2$	$P_1 (\nabla \cdot \nabla) \boldsymbol{\theta} + P_2 \nabla (\nabla \cdot \boldsymbol{\theta}) + Q (\nabla w - \boldsymbol{\theta}) = \mathbf{0}$ $Q (\nabla \cdot \nabla w - \nabla \cdot \boldsymbol{\theta}) + q = 0$
Matrix Form $[\mathbf{L}] \{\mathbf{u}\} + \{\mathbf{b}\} = \mathbf{0}$	$[\mathbf{L}] = \nabla^2$ $\{\mathbf{u}\} = u$ $\{\mathbf{b}\} = b$	$[\mathbf{L}] = [\hat{\nabla}]^T [\mathbf{D}] [\hat{\nabla}]$ $\{\mathbf{u}\} = \{u_1, u_2, u_3\}^T$ $\{\mathbf{b}\} = \{b_1, b_2, b_3\}^T$	$[\mathbf{L}] = \begin{Bmatrix} [\bar{\nabla}]^T [\mathbf{G}] + [\mathbf{D}^s] [\mathbf{N}] \\ [\bar{\nabla}]^T [\mathbf{D}^s] [\mathbf{N}] \end{Bmatrix}$ $\{\mathbf{u}\} = \{\theta_1, \theta_2, w\}^T$ $\{\mathbf{b}\} = \{0, 0, q\}^T$
Fund. Sol. $\mathbf{g}(\mathbf{x}, \bar{\mathbf{x}})$	$g(\mathbf{x}, \bar{\mathbf{x}}) = -\frac{1}{2\pi} \ln r$ $r = \sqrt{\sum_{i=1}^n (x_i - \bar{x}_i)^2}$	$g_{ij}(\mathbf{x}, \bar{\mathbf{x}}) = \frac{1}{16\pi\mu(1-\nu)r} \times [(3-4\nu)\delta_{ij} + r_{,i}r_{,j}]$ $r_{,j} = \frac{\partial r}{\partial x_j}$	$g_{13}(\mathbf{x}, \bar{\mathbf{x}}) = \frac{1}{8\pi D} r(2 \ln r + 1) \cos(\mathbf{r}, \mathbf{x}_1)$ $g_{23}(\mathbf{x}, \bar{\mathbf{x}}) = \frac{1}{8\pi D} r(2 \ln r + 1) \sin(\mathbf{r}, \mathbf{x}_1)$ $g_{33}(\mathbf{x}, \bar{\mathbf{x}}) = \frac{1}{8\pi D} r^2 \ln r - \frac{1}{2\pi Q} \ln r$ $g_{ij} = 0 \quad \text{for } j \neq 3$
Part.Sol. $\mathbf{u}^p(\mathbf{x})$	$u^p(\bar{\mathbf{x}}) = \int_{\Omega} g(\mathbf{x}, \mathbf{y}) b(\mathbf{y}) d\mathbf{y}$	$u_i^p(\mathbf{x}) = \int_{\Omega} g_{ij}(\mathbf{x}, \mathbf{y}) b_j(\mathbf{y}) d\mathbf{y}$	$u_i^p(\mathbf{x}) = \int_{\Omega} g_{ij}(\mathbf{x}, \mathbf{y}) b_j(\mathbf{y}) d\mathbf{y}$

Note: $P_1, P_2, Q, D, [\hat{\nabla}], [\bar{\nabla}], [\mathbf{D}^s], [\mathbf{G}], [\mathbf{N}]$ in Table 1 are defined in Appendix.

2.3 A Stabilized Conforming Nodal Integration for Homogeneous Solution

The variable $\mathbf{u}^0(\mathbf{x})$ satisfying Eq. (15) without a source term involves a lower order behavior compared with the original problem and can be effectively solved numerically. It has been studied by Chen et al. [7, 8] that the necessary conditions for achieving linear exactness in the Galerkin approximation of second order differential equations are: (1) shape functions Ψ_I for approximation of the unknown $u_i^h(\mathbf{x}) = \sum_{I=1}^{NP} \Psi_I(\mathbf{x}) d_{iI}$ are linearly complete, and (2) integration of the weak form meets the following integration constraint:

$$Int_{\Omega}(\nabla\Psi_I) = \int_{\partial_h\Omega} \Psi_I \mathbf{n} d\Gamma \text{ for } \{I : supp(\Psi_I) \cap \partial_u\Omega = \emptyset\} \quad (16)$$

where $Int_{\Omega}(\cdot)$ denotes numerical integration over domain Ω and \mathbf{n} is the surface normal on $\partial_h\Omega$. A stabilized conforming nodal integration (SCNI) has been proposed to stabilize the nodal integration of the weak form and fulfill linear exactness in the Galerkin approximation of second order differential equation [7]. In this approach, a smoothed nodal gradient of u at point \mathbf{x}_L is computed as:

$$\tilde{\nabla}u^h(\mathbf{x}_L) = \frac{1}{A_L} \int_{\Omega_L} \nabla u^h dA = \frac{1}{A_L} \int_{\Gamma_L} \mathbf{n} u^h d\Gamma = \sum_I \tilde{\nabla}\Psi_I(\mathbf{x}_L) d_I \quad (17)$$

where

$$\tilde{\nabla}\Psi_I(\mathbf{x}_L) = \frac{1}{A_L} \int_{\Gamma_L} \Psi_I(\mathbf{x}) \mathbf{n}(\mathbf{x}) d\Gamma \quad (18)$$

Here Ω_L and Γ_L are the representative domain and boundary associated with the node L as shown in Fig. 3, and A_L is the area (or volume) of Ω_L . It can be easily shown that this smoothed gradient meets the integration constraints for nodal integration:

$$Int_{\Omega}(\tilde{\nabla}\Psi_I) = \sum_{L=1}^{NP} \tilde{\nabla}\Psi_I(\mathbf{x}_L) A_L = \int_{\partial_h\Omega} \Psi_I \mathbf{n} d\Gamma \text{ for } \{I : supp(\Psi_I) \cap \partial_u\Omega = \emptyset\} \quad (19)$$

This SCNI method will be employed in the integration of weak form of the homogeneous solution for Poisson, elasticity, and Mindlin-Reissner problems in the next Section.

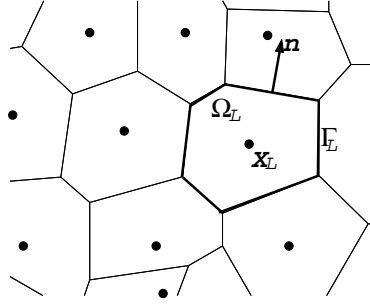


Fig. 3. Nodal representative domain obtained by Voronoi diagram

3 Extended Meshfree Method for Elastic Boundary Value Problems

In this section we discuss the extended meshfree solution procedure when the particular solutions are obtained in Section 2. The construction of discrete equations for the homogeneous solution of Poisson, elasticity, and Mindlin-Reissner plate problems is also summarized. To distinguish from the tensor notation, matrix and vector are denoted by “[.]” and “{.}” symbols, respectively, in the following discussion.

3.1 Poisson Problem

Consider a Poisson problem in Table 1 with boundary conditions $u = g$ on $\partial_u \Omega$ and $\partial u / \partial n = h$ on $\partial_h \Omega$. The weak form of the homogeneous solution of Poisson problem is:

$$\begin{aligned} \int_{\Omega} \nabla \delta u^0 \cdot \nabla u^0 d\Omega &= \int_{\partial_h \Omega} \delta u^0 \left(h - \frac{\partial u^p}{\partial n} \right) d\Gamma \\ u^0 &= g - u^p \quad \text{on} \quad \partial_u \Omega \end{aligned} \quad (20)$$

Introducing a nodal integration of weak form with assumed gradient field (17) into Eq. (20) yields:

$$\sum_{L=1}^{NP} \tilde{\nabla} \delta u^0(\mathbf{x}_L) \cdot \tilde{\nabla} u^0(\mathbf{x}_L) A_L = \sum_{K=1}^{NB_{int}} \delta u^0(\bar{\mathbf{x}}_K) \left(h(\bar{\mathbf{x}}_K) - \frac{\partial u^p}{\partial n}(\bar{\mathbf{x}}_K) \right) \varpi_K \quad (21)$$

where NP and NB_{int} are the numbers of nodal points and boundary integration points, respectively, and $\bar{\mathbf{x}}_L$ and ϖ_K are the integration points and weights for boundary integration, respectively, which are consistent with the boundary integration for gradient smoothing term $\int_{\Gamma_L} \Psi_I(\mathbf{x}) \mathbf{n}(\mathbf{x}) d\Gamma$ in Eq. (18). By substituting the meshfree approximation for $u^{0h}(\mathbf{x}) = \sum_{I=1}^{NP} \Psi_I(\mathbf{x}) d_I^0$ into Eq. (21), we obtain the following discrete equation for homogeneous solution:

$$[\mathbf{K}] \{ \mathbf{d}^0 \} = \{ \mathbf{f}^0 \} \quad (22)$$

$$K_{IJ} = \sum_{L=1}^{NP} \left\{ \tilde{\mathbf{b}}_I(\mathbf{x}_L) \right\}^T \left\{ \tilde{\mathbf{b}}_J(\mathbf{x}_L) \right\} A_L \quad (23)$$

$$\left\{ \tilde{\mathbf{b}}_I(\mathbf{x}_L) \right\} = \left\{ \begin{array}{c} \tilde{b}_{1I}(\mathbf{x}_L) \\ \tilde{b}_{2I}(\mathbf{x}_L) \end{array} \right\} \quad (24)$$

$$\tilde{b}_{iI}(\mathbf{x}_L) = \frac{1}{A_L} \int_{\Gamma_L} \Psi_I(\mathbf{x}) n_i(\mathbf{x}) d\Gamma \quad (25)$$

$$f_I^0 = \sum_{K=1}^{NBint} \Psi_I(\bar{\mathbf{x}}_K) \left(h(\bar{\mathbf{x}}_K) - \frac{\partial u^p}{\partial n}(\bar{\mathbf{x}}_K) \right) \varpi_K \quad (26)$$

Problem (7) is revisited using the aforementioned Extended-RKPM. The particular solution of this problem in Table 1 is computed using three integration zones with 6-point quadrature rule in the small domain where $b(x) \neq 0$, and the homogeneous solution is obtained by RKPM with SCNI. The comparison of the results in Fig. 4 shows a significant improvement in solution accuracy using the Extended-RKPM compared to SC-RKPM in Fig. 3. Note that since the particular solution is obtained analytically, the solution error is independent to the source term localization parameter α .

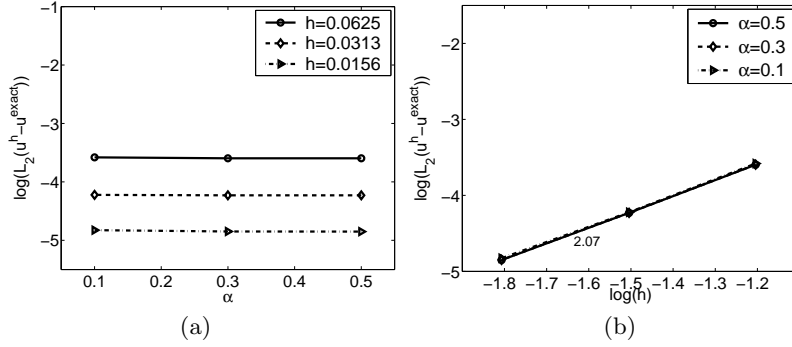


Fig. 4. Effects of discretization and source term localization on L_2 error norm of u in problem (7) using Extend-RKPM

3.2 Elasticity

Consider an elasticity problem in Table 1 with boundary conditions $u_i = g_i$ on $\partial_u \Omega$ and $(\mathbf{C} : (\nabla^s \mathbf{u})) \cdot \mathbf{n} = \mathbf{h}$ on $\partial_h \Omega$. The weak form of the homogeneous solution of elasticity problem is:

$$\int_{\Omega} (\nabla^s \delta \mathbf{u}^0) : \mathbf{C} : (\nabla^s \mathbf{u}^0) d\Omega = \int_{\partial_h \Omega} \delta \mathbf{u}^0 \cdot (\mathbf{h} - (\mathbf{C} : (\nabla^s \mathbf{u}^p)) \cdot \mathbf{n}) d\Gamma \quad (27)$$

$$u_i^0 = g_i - u_i^p \quad \text{on} \quad \partial_u \Omega$$

Similar to the smoothing of ∇u^0 in Poisson problem, the strain corresponding to \mathbf{u}^0 is smoothed in elasticity. Let

$$\varepsilon_{ij}^0 = (\nabla^s \mathbf{u}^0)_{ij} = \frac{1}{2} (u_{i,j}^0 + u_{j,i}^0) \quad (28)$$

The smoothed strain of \mathbf{u}^0 at point \mathbf{x}_L is obtained by

$$\begin{aligned} \tilde{\varepsilon}_{ij}^0(\mathbf{x}_L) &= \frac{1}{A_L} \int_{\Omega_L} \varepsilon_{ij}^0 dA = \frac{1}{2A_L} \int_{\Omega_L} (u_{i,j}^0 + u_{j,i}^0) dA \\ &= \frac{1}{2A_L} \int_{\Gamma_L} (u_i^0 n_j + u_j^0 n_i) d\Gamma \end{aligned} \quad (29)$$

Defining a smoothed strain vector $\{\tilde{\boldsymbol{\varepsilon}}^0\} = \{\tilde{\varepsilon}_{11}^0, \tilde{\varepsilon}_{22}^0, 2\tilde{\varepsilon}_{12}^0\}^T$ and introducing MLS/RK approximation for $u_i^{0h}(\mathbf{x}) = \sum_{I=1}^{NP} \Psi_I(\mathbf{x}) d_{iI}^0$ in Eq. (29), we have

$$\{\tilde{\boldsymbol{\varepsilon}}^{0h}(\mathbf{x}_L)\} = \sum_{I=1}^{NP} [\tilde{\mathbf{B}}_I(\mathbf{x}_L)] \{\mathbf{d}_I^0\} \quad (30)$$

where

$$[\tilde{\mathbf{B}}_I(\mathbf{x}_L)] = \begin{bmatrix} \tilde{b}_{I1}(\mathbf{x}_L) & 0 \\ 0 & \tilde{b}_{I2}(\mathbf{x}_L) \\ \tilde{b}_{I2}(\mathbf{x}_L) & \tilde{b}_{I1}(\mathbf{x}_L) \end{bmatrix}, \quad \{\mathbf{d}_I^0\} = \begin{Bmatrix} d_{1I}^0 \\ d_{2I}^0 \end{Bmatrix} \quad (31)$$

and $\tilde{b}_{iI}(\mathbf{x}_L)$ is defined in Eq. (25). Introducing a nodal integration to the weak form of elasticity in Eq. (27) with smoothed strain field defined in Eq. (29) yields the following stiffness matrix and force vector for solving the homogeneous solution $[\mathbf{K}] \{\mathbf{d}^0\} = \{\mathbf{f}^0\}$:

$$[\mathbf{K}_{IJ}] = \sum_{L=1}^{NP} [\tilde{\mathbf{B}}_I(\mathbf{x}_L)]^T [\mathbf{D}] [\tilde{\mathbf{B}}_J(\mathbf{x}_L)] A_L \quad (32)$$

$$\{\mathbf{f}_I^0\} = \sum_{K=1}^{NB_{int}} \Psi_I(\bar{\mathbf{x}}_K) \begin{Bmatrix} h_1(\bar{\mathbf{x}}_K) - \sigma_{1j}^p(\bar{\mathbf{x}}_K) n_j(\bar{\mathbf{x}}_K) \\ h_2(\bar{\mathbf{x}}_K) - \sigma_{2j}^p(\bar{\mathbf{x}}_K) n_j(\bar{\mathbf{x}}_K) \end{Bmatrix} \varpi_K \quad (33)$$

where $\boldsymbol{\sigma}^p = \mathbf{C} : \nabla^s \mathbf{u}^p$, and $[\mathbf{D}]$ is the matrix form of the elasticity tensor \mathbf{C} .

A cantilever beam subjected to a tip shear force shown in Fig. 5(a) is analyzed using SC-RKPM (RKPM with stabilized conforming nodal integration), G-RKPM (RKPM with Gauss integration) and Extended-RKPM. The geometry and material properties are; $L=10$, $D=2$, $E=21\text{MPa}$, $\nu=0.3$. The total shear load is 1, which is distributed in a parabolic function over the depth of the free end. Three discretizations as shown in Fig. 5(b) are employed to compute error in the numerical solution. The SCNI is employed for the total solution in SC-RKPM and the homogeneous solution of Extended-RKMP as discussed above. In Extended-RKPM, the shear force is treated as a source term with distributed load, and the fundamental solution in Table 1 is used to calculate the particular solution. Figure 5(c) shows that the Extended-RKPM

greatly reduces the L_2 error norm of \mathbf{u} compared to those of SC-RKPM and G-RKPM.

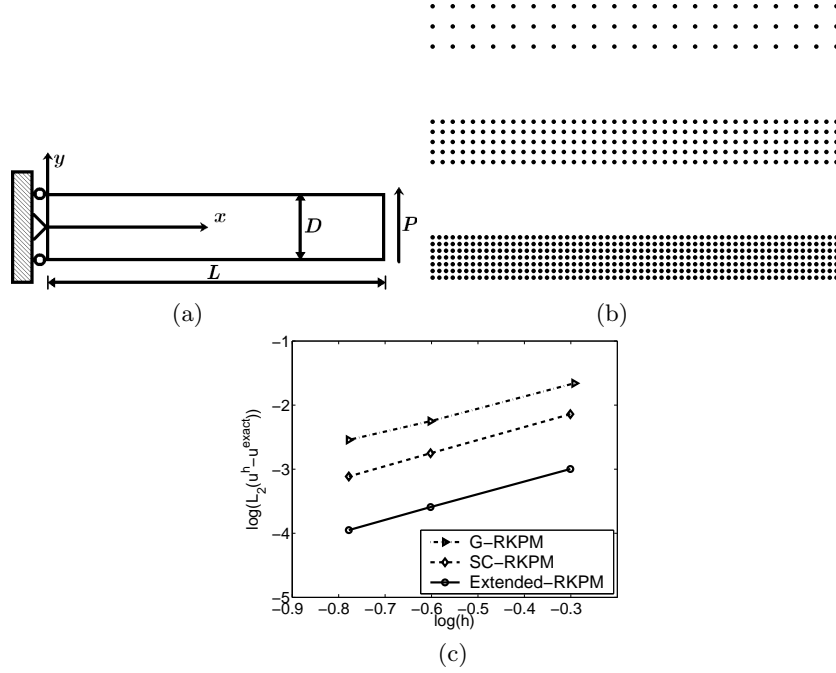


Fig. 5. Beam problem solved by various methods: (a) problem description; (b) discretizations; (c) L_2 error norm of u

3.3 Mindlin-Reissner Plate Problem

Consider a Mindlin-Reissner plate problem in Table 1 with boundary conditions $\theta_\alpha = \bar{\theta}_\alpha$ ($\alpha = 1, 2$), $w = \bar{w}$ on $\partial_u \Omega$ and $(\mathbf{C}^b : (\nabla^s \boldsymbol{\theta})) \cdot \mathbf{n} = \bar{\mathbf{m}}$ on $\partial_h \Omega$. The weak form of the homogeneous part of Mindlin-Reissner problem given in Table 1 can be expressed as

$$\begin{aligned}
 & \int_{\Omega} \nabla^s \delta \boldsymbol{\theta}^0 : \mathbf{C}^b : \nabla^s \boldsymbol{\theta}^0 d\Omega + \int_{\Omega} (\nabla \delta w^0 - \delta \boldsymbol{\theta}^0) : \mathbf{C}^s : (\nabla w^0 - \boldsymbol{\theta}^0) d\Omega \\
 & + \int_{\partial_h \Omega} \delta \boldsymbol{\theta}^0 \cdot (\bar{\mathbf{m}} - (\mathbf{C}^b : (\nabla^s \boldsymbol{\theta}^p)) \cdot \mathbf{n}) d\Gamma = 0 \\
 & \theta_\alpha = \bar{\theta}_\alpha, \quad w = \bar{w}, \quad \text{on} \quad \partial_u \Omega
 \end{aligned} \tag{34}$$

where \mathbf{C}^b and \mathbf{C}^s are the elasticity moduli for bending and shear, respectively. To meet integration constraint and provide stability to the nodally integrated

weak form of Eq. (34), a curvature smoothing at the nodal point is introduced [24]. Let curvature of the homogeneous solution be denoted as

$$k_{\alpha\beta}^0 = (\nabla^s \theta^0)_{\alpha\beta} = \frac{1}{2} (\theta_{\alpha,\beta}^0 + \theta_{\beta,\alpha}^0) \quad (35)$$

The smoothed curvature at point \mathbf{x}_L is obtained by

$$\begin{aligned} \tilde{\kappa}_{\alpha\beta}^0(\mathbf{x}_L) &= \frac{1}{A_L} \int_{\Omega_L} \kappa_{\alpha\beta}^0(\mathbf{x}) dA = \frac{1}{2A_L} \int_{\Omega_L} (\theta_{\alpha,\beta}^0 + \theta_{\beta,\alpha}^0) dA \\ &= \frac{1}{2A_L} \int_{\Gamma_L} (\theta_{\alpha}^0 n_{\beta} + \theta_{\beta}^0 n_{\alpha}) d\Gamma \end{aligned} \quad (36)$$

Introducing MLS/RK to the approximation of $\theta_{\alpha}^{0h}(\mathbf{x}) = \sum_{I=1}^{NP} \Psi_I(\mathbf{x}) \theta_{\alpha I}^0$ and $w^{0h}(\mathbf{x}) = \sum_{I=1}^{NP} \Psi_I(\mathbf{x}) w_I^0$ in smoothed curvature $\{\tilde{\boldsymbol{\kappa}}^0\} = \{\tilde{\kappa}_{11}^0, \tilde{\kappa}_{22}^0, 2\tilde{\kappa}_{12}^0\}^T$ and shear strain $\{\boldsymbol{\gamma}^0\} = \{w_{,1}^0 - \theta_1^0, w_{,2}^0 - \theta_2^0\}^T$, we have

$$\{\tilde{\boldsymbol{\kappa}}^{0h}\} = \sum_{I=1}^{NP} [\tilde{\mathbf{B}}_I^b] \{\mathbf{d}_I^0\}, \quad \{\boldsymbol{\gamma}^{0h}\} = \sum_{I=1}^{NP} [\mathbf{B}_I^s] \{\mathbf{d}_I^0\} \quad (37)$$

$$[\tilde{\mathbf{B}}_I^b] = \begin{bmatrix} 0 & \tilde{b}_{I1} & 0 \\ 0 & 0 & \tilde{b}_{I2} \\ 0 & \tilde{b}_{I2} & \tilde{b}_{I1} \end{bmatrix}, \quad [\mathbf{B}_I^s] = \begin{bmatrix} \Psi_{I,x} & -\Psi_I & 0 \\ \Psi_{I,y} & 0 & -\Psi_I \end{bmatrix}, \quad \{\mathbf{d}_I^0\} = \begin{Bmatrix} w_I^0 \\ \theta_{1I}^0 \\ \theta_{2I}^0 \end{Bmatrix} \quad (38)$$

Introducing a nodal integration to weak form in Eq. (34) with smoothed curvature in Eq. (37) yields the following stiffness matrix and force vector for solving the homogeneous solution $[\mathbf{K}] \{\mathbf{d}^0\} = \{\mathbf{f}^0\}$:

$$[\mathbf{K}] = [\mathbf{K}^b] + [\mathbf{K}^s] \quad (39)$$

$$[\mathbf{K}_{IJ}^b] = \sum_{L=1}^{NP} [\tilde{\mathbf{B}}_I^b(\mathbf{x}_L)]^T [\mathbf{D}^b] [\tilde{\mathbf{B}}_J^b(\mathbf{x}_L)] A_L \quad (40)$$

$$[\mathbf{K}_{IJ}^s] = \sum_{L=1}^{NP} [\mathbf{B}_I^s(\mathbf{x}_L)]^T [\mathbf{D}^s] [\mathbf{B}_J^s(\mathbf{x}_L)] A_L$$

$$\{\mathbf{f}_I^0\} = \sum_{K=1}^{NB_{int}} \Psi_I(\bar{\mathbf{x}}_K) \begin{Bmatrix} 0 \\ m_{1\alpha}^p(\bar{\mathbf{x}}_K) n_{\alpha}(\bar{\mathbf{x}}_K) - \bar{m}_1(\bar{\mathbf{x}}_K) \\ m_{2\alpha}^p(\bar{\mathbf{x}}_K) n_{\alpha}(\bar{\mathbf{x}}_K) - \bar{m}_2(\bar{\mathbf{x}}_K) \end{Bmatrix} \varpi_K \quad (41)$$

where $\mathbf{m}^p = \mathbf{C}^b : \nabla^s \boldsymbol{\theta}^p$, $[\mathbf{D}^b]$ and $[\mathbf{D}^s]$ are the matrix forms of \mathbf{C}^b and \mathbf{C}^s tensors, respectively.

A clamped circular plate subjected to a unit concentrated load P at the plate centroid shown in Fig. 6(a) is analyzed. Since the source term is due to a point load, the particular solution is the fundamental solution. RKPM with

SCNI (SC-RKPM), RKPM with Gauss integration (G-RKPM) and Extended-RKPM discussed above using three discretizations shown in Fig. 6(b) are compared in Fig. 6(c). A substantial improvement of the solution accuracy in Extended-RKPM over G-RKPM and SC-RKPM is achieved.

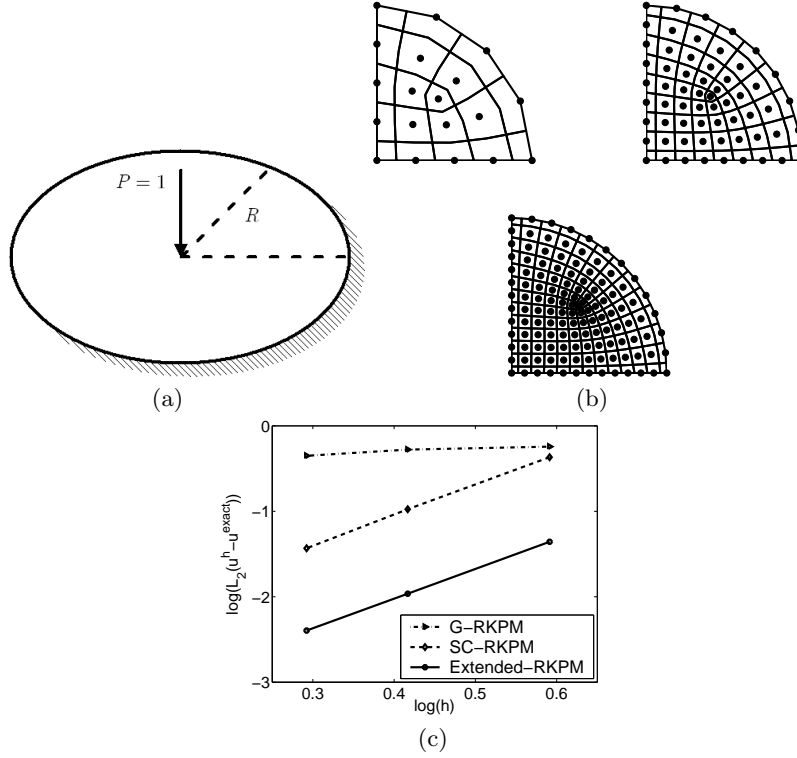


Fig. 6. Mindlin-Reissner plate solved by various methods:(a) problem description; (b) discretizations; (c) L_2 error norm of \mathbf{u}

4 Extended Meshfree Method for Inelastic Boundary Value Problems

4.1 Self-Adjoint Operator

Here we consider BVP in Eq. (8), with \mathcal{L} the differential operator for inelastic media which, in general, is a nonlinear operator, i.e., $\mathcal{L}(\mathbf{u}^0 + \mathbf{u}^p) \neq \mathcal{L}(\mathbf{u}^0) + \mathcal{L}(\mathbf{u}^p)$. To start, express the weak form of BVP as

$$\int_{\Omega} \mathbf{v} \cdot \mathcal{L}(\mathbf{u}) d\Omega + \int_{\Omega} \mathbf{v} \cdot \mathbf{b} d\Omega = 0 \quad (42)$$

where \mathbf{v} is the weight function and $\mathbf{v} = \mathbf{0}$ on essential boundary $\partial_u \Omega$. If \mathcal{L} is self-adjoint, then we have

$$\int_{\Omega} \mathbf{v} \cdot \mathcal{L}(\mathbf{u}) d\Omega = \int_{\Omega} \mathbf{u} \cdot \mathcal{L}(\mathbf{v}) d\Omega + \int_{\Omega} \sum_i \mathcal{B}_i(\mathbf{u}, \mathbf{v}) d\Gamma \quad (43)$$

where the 2^{nd} term on the right hand side of Eq. (43) is a boundary term resulting from integration by parts, and \mathcal{B}_i are the corresponding boundary operators. Thus Eq. (42) can be expressed as

$$\int_{\Omega} \mathbf{u} \cdot \mathcal{L}(\mathbf{v}) d\Omega + \int_{\Omega} \mathbf{v} \cdot \mathbf{b} d\Omega + \int_{\partial\Omega} \sum_i \mathcal{B}_i(\mathbf{u}, \mathbf{v}) d\Gamma = 0 \quad (44)$$

By deposition of unknown $\mathbf{u} = \mathbf{u}^p + \mathbf{u}^0$, we have

$$\int_{\Omega} \mathbf{u}^0 \cdot \mathcal{L}(\mathbf{v}) d\Omega + \int_{\Omega} \mathbf{u}^p \cdot \mathcal{L}(\mathbf{v}) d\Omega + \int_{\Omega} \mathbf{v} \cdot \mathbf{b} d\Omega + \int_{\partial\Omega} \sum_i \mathcal{B}_i(\mathbf{u}, \mathbf{v}) d\Gamma = 0 \quad (45)$$

Since \mathcal{L} is a self-adjoint differential operator, the first 2 terms on the left hand side of Eq. (45) can be transformed according to Eq. (43) to yield

$$\begin{aligned} & \int_{\Omega} \mathbf{v} \cdot \mathcal{L}(\mathbf{u}^0) d\Omega + \int_{\Omega} \mathbf{v} \cdot \mathcal{L}(\mathbf{u}^p) d\Omega + \int_{\Omega} \mathbf{v} \cdot \mathbf{b} d\Omega \\ & + \int_{\partial\Omega} \sum_i (\mathcal{B}_i(\mathbf{v}, \mathbf{u}^0) + \mathcal{B}_i(\mathbf{v}, \mathbf{u}^p) + \mathcal{B}_i(\mathbf{u}, \mathbf{v})) d\Gamma = 0 \end{aligned} \quad (46)$$

If a particular solution for $\mathcal{L}(\mathbf{u}^p) + \mathbf{b} = \mathbf{0}$ exists, Eq. (46) is reduced to the following problem:

$$\int_{\Omega} \mathbf{v} \cdot \mathcal{L}(\mathbf{u}^0) d\Omega + \int_{\partial\Omega} \sum_i (\mathcal{B}_i(\mathbf{u}, \mathbf{v}) + \mathcal{B}_i(\mathbf{v}, \mathbf{u}^0) + \mathcal{B}_i(\mathbf{v}, \mathbf{u}^p)) d\Gamma = 0 \quad (47)$$

Equation (47) leads to the following strong form:

$$\mathcal{L}(\mathbf{u}^0) = \mathbf{0} \quad (48)$$

with natural boundary conditions:

$$\begin{aligned} & \sum_i (\mathcal{B}_i(\mathbf{u}^0 + \mathbf{u}^p, \mathbf{v}) + \mathcal{B}_i(\mathbf{v}, \mathbf{u}^0) + \mathcal{B}_i(\mathbf{v}, \mathbf{u}^p)) = \mathbf{0} \\ & \text{for arbitrary } \mathbf{v} \text{ with } \mathbf{v} = \mathbf{0} \text{ on } \partial_u \Omega \end{aligned} \quad (49)$$

For a given \mathbf{u}^p , Eq. (49) gives the natural boundary conditions for the homogeneous solution \mathbf{u}^0 . Further, Eq. (46) provides the weak form for solving \mathbf{u}^0 .

4.2 Elasto-plasticity Problem

Consider the following elasto-plasticity problem:

$$\begin{aligned}
 \nabla \cdot \dot{\boldsymbol{\sigma}} + \dot{\mathbf{b}} &= \mathbf{0} \quad \text{in } \Omega_x \\
 \dot{\boldsymbol{\sigma}} &= \mathbf{C}^e : \dot{\boldsymbol{\varepsilon}}^e = \mathbf{C}^* : \dot{\boldsymbol{\varepsilon}} \\
 \dot{\boldsymbol{\varepsilon}} &= \nabla^s \dot{\mathbf{u}} = \dot{\boldsymbol{\varepsilon}}^e + \dot{\boldsymbol{\varepsilon}}^* \\
 \mathbf{u} &= \hat{\mathbf{u}} \quad \text{on } \partial_u \Omega_x, \\
 \dot{\boldsymbol{\sigma}} \cdot \mathbf{n} &= \dot{\mathbf{h}} \quad \text{on } \partial_h \Omega_x
 \end{aligned} \tag{50}$$

where Ω_x is the deformed configuration, \mathbf{C}^e and \mathbf{C}^* are elastic and elasto-plastic moduli, respectively, $\dot{\boldsymbol{\varepsilon}}^e$ and $\dot{\boldsymbol{\varepsilon}}^*$ are elastic and plastic strain rates, respectively, ∇^s is the symmetric gradient operator, i.e., $(\nabla^s \dot{\mathbf{u}})_{ij} = (\dot{u}_{i,j} + \dot{u}_{j,i})/2$, $\dot{\boldsymbol{\sigma}}$ is the Cauchy stress rate, \mathbf{n} is the normal unit vector of traction surface, and $\dot{\mathbf{h}}$ is the surface traction rate. For elasto-plastic materials that obey associative flow rule, we have:

$$\dot{\boldsymbol{\varepsilon}}^* = \dot{\gamma} \frac{\partial f}{\partial \boldsymbol{\sigma}} \tag{51}$$

where f is the yield function and $\dot{\gamma}$ denotes the plastic consistency parameter.

To employ the extended meshfree method discussed earlier, Eq. (50) is recast into the following form:

$$\underbrace{\nabla \cdot (\mathbf{C}^e : \nabla^s \dot{\mathbf{u}})}_{\mathcal{L}(\dot{\mathbf{u}})} + \underbrace{(\dot{\mathbf{b}} - \nabla \cdot (\mathbf{C}^* : \dot{\boldsymbol{\varepsilon}}^*))}_{\text{source}} = \mathbf{0} \tag{52}$$

Here the nonlinearity is included in the source term. The solution is solved as follows:

1. Particular solution

$$\dot{u}_i^p(\mathbf{x}) = \int_{\Omega_x} g_{ij}(\mathbf{x}, \mathbf{y}) \left(\dot{b}_j(\mathbf{y}) - \frac{\partial (C_{j m k l}^e \dot{\varepsilon}_{k l}^*(\mathbf{y}))}{\partial y_m} \right) d\mathbf{y} \tag{53}$$

where g_{ij} is the fundamental solution associated with the differential operator $\mathcal{L}(\dot{\mathbf{u}}) = \nabla \cdot (\mathbf{C}^e : \nabla^s \dot{\mathbf{u}})$, and the particular solution \dot{u}_i^p is computed at every time step. The integration of Eq. (53) is performed over the deformed configuration Ω_x .

2. Homogeneous problem:

$$\begin{aligned}
 \nabla \cdot (\mathbf{C}^e : \nabla^s \dot{\mathbf{u}}^0) &= \mathbf{0} \quad \text{in } \Omega \\
 \mathbf{u}^0 &= \hat{\mathbf{u}} - \mathbf{u}^p \quad \text{on } \partial_u \Omega, \\
 \dot{\boldsymbol{\sigma}}^0 \cdot \mathbf{n} &= \dot{\mathbf{h}} - (\mathbf{C}^* : \nabla^s \dot{\mathbf{u}}^p) \cdot \mathbf{n} \quad \text{on } \partial_h \Omega
 \end{aligned} \tag{54}$$

where $\dot{\boldsymbol{\sigma}}^0 = (\mathbf{C}^* : \nabla^s \dot{\mathbf{u}}^0) \cdot \mathbf{n}$ is the Cauchy stress rate associated with the homogeneous solution $\dot{\mathbf{u}}^0$.

Note that the homogeneous solution in Eq. (54) is almost identical to the homogeneous solution of elasticity, except for the corrected natural boundary condition involving elasto-plastic moduli. Thus the meshfree approximation and SCNI for domain integration used in elasticity are directly applicable to this case.

Remarks:

An alternative approach for solving problem (50) is to consider the following strong form:

$$\underbrace{\nabla \cdot (\mathbf{C}^* : \nabla^s \dot{\mathbf{u}})}_{\mathcal{L}(\dot{\mathbf{u}})} + \dot{\mathbf{b}} = \mathbf{0} \quad (55)$$

Here, the elasto-plastic moduli \mathbf{C}^* reside in the differential operator. We consider the weak form of Eq. (55)

$$\int_{\Omega} \mathbf{v} \cdot (\nabla \cdot (\mathbf{C}^* : \nabla^s \dot{\mathbf{u}})) d\Omega + \int_{\Omega} \mathbf{v} \cdot \dot{\mathbf{b}} d\Omega = 0 \quad (56)$$

where the weight function $\mathbf{v} = \mathbf{0}$ on $\partial\Omega_u$. Via integration by parts and divergence theorem, we have

$$\begin{aligned} & \int_{\partial_h \Omega} \mathbf{v} \cdot \dot{\mathbf{h}} d\Gamma - \int_{\partial_h \Omega} \dot{\mathbf{u}} \cdot (\nabla^s \mathbf{v} : \mathbf{C}^* \cdot \mathbf{n}) d\Gamma + \int_{\Omega} \dot{\mathbf{u}} \cdot (\nabla \cdot (\mathbf{C}^* : \nabla^s \mathbf{v})) d\Omega \\ & + \int_{\Omega} \mathbf{v} \cdot \dot{\mathbf{b}} d\Omega = 0 \end{aligned} \quad (57)$$

Note that we have used the properties $C_{ijkl}^* = C_{klij}^* = C_{jikl}^* = C_{ijlk}^*$. Next, by the decomposition of $\dot{\mathbf{u}} = \dot{\mathbf{u}}^p + \dot{\mathbf{u}}^0$, we have

$$\begin{aligned} & \int_{\Omega} \dot{\mathbf{u}} \cdot (\nabla \cdot (\mathbf{C}^* : \nabla^s \mathbf{v})) d\Omega \\ & = \int_{\Omega} \dot{\mathbf{u}}^p \cdot (\nabla \cdot (\mathbf{C}^* : \nabla^s \mathbf{v})) d\Omega + \int_{\Omega} \dot{\mathbf{u}}^0 \cdot (\nabla \cdot (\mathbf{C}^* : \nabla^s \mathbf{v})) d\Omega \end{aligned} \quad (58)$$

Further applying integration by parts, the following equation can be obtained

$$\begin{aligned} & \int_{\Omega} \mathbf{v} \cdot (\nabla \cdot (\mathbf{C}^* : \nabla^s \dot{\mathbf{u}}^p)) d\Omega + \int_{\Omega} \mathbf{v} \cdot (\nabla \cdot (\mathbf{C}^* : \nabla^s \dot{\mathbf{u}}^0)) d\Omega + \int_{\partial_h \Omega} \mathbf{v} \cdot \dot{\mathbf{h}} d\Omega \\ & - \int_{\partial_h \Omega} \mathbf{v} \cdot ((\mathbf{C}^* : \nabla^s \dot{\mathbf{u}}^p) \cdot \mathbf{n}) d\Gamma + \int_{\Omega} \mathbf{v} \cdot \dot{\mathbf{b}} d\Omega = 0 \end{aligned} \quad (59)$$

In the typical incremental solution procedure, \mathbf{C}^* is formed with solution of the previous time step. Thus if the fundamental solution of differential operator in Eq. (55) with an explicit \mathbf{C}^* exists, Eq. (59) can be reduced to

$$\int_{\partial_h \Omega} \mathbf{v} \cdot (\dot{\mathbf{h}} - (\mathbf{C}^* : \nabla^s \dot{\mathbf{u}}^p) \cdot \mathbf{n}) d\Gamma + \int_{\Omega} \mathbf{v} \cdot (\nabla \cdot (\mathbf{C}^* : \nabla^s \dot{\mathbf{u}}^0)) d\Omega = 0 \quad (60)$$

This leads to the following strong form and natural boundary conditions for the homogeneous solution:

$$\begin{aligned} \nabla \cdot (\mathbf{C}^* : \nabla^s \dot{\mathbf{u}}^0) &= \mathbf{0} \quad \text{in } \Omega \\ (\mathbf{C}^* : \nabla^s \dot{\mathbf{u}}^0) \cdot \mathbf{n} &= \dot{\mathbf{h}} - (\mathbf{C}^* : \nabla^s \dot{\mathbf{u}}^p) \cdot \mathbf{n} \quad \text{on } \partial_h \Omega \end{aligned} \quad (61)$$

The corresponding weak form of Eq. (61) is

$$\int_{\Omega} \nabla^s \mathbf{v} : \mathbf{C}^* : \nabla^s \dot{\mathbf{u}}^0 d\Omega = \int_{\partial_h \Omega} \mathbf{v} \cdot (\dot{\mathbf{h}} - (\mathbf{C}^* : \nabla^s \dot{\mathbf{u}}^p) \cdot \mathbf{n}) d\Gamma \quad (62)$$

4.3 Some Remarks on Consideration of Large Deformation

In the case where the materials undergo large deformation, the undeformed configuration Ω_X and deformed configuration Ω_x of the material domain need to be distinguished. Considering a material point $\mathbf{X} \in \Omega_X$ under deformation is moved to $\mathbf{x} \in \Omega_x$, where Ω_X is the undeformed configuration and Ω_x is the corresponding deformed configuration, and $\mathbf{x} = \mathbf{X} + \mathbf{u}$, where \mathbf{u} is the displacement. For a general nonlinear problem, incremental solution procedures are required, and the incremental equation of Eq. (52) is solved:

$$\underbrace{\nabla \cdot (\mathbf{C}^e : \nabla^s \Delta \mathbf{u})}_{\mathcal{L}(\Delta \mathbf{u})} + \underbrace{(\Delta \mathbf{b} - \nabla \cdot (\mathbf{C}^e : \Delta \varepsilon^*))}_{\text{source}} = \Delta \mathbf{r} \quad (63)$$

where "Δ" denote a finite increment quantity, and $\Delta \mathbf{r}$ is the residual. The increment of particular solution Δu_i^p is obtained by

$$\Delta u_i^p(x) = \int_{\Omega_x} g_{ij}(\mathbf{x}, \mathbf{y}) \left(\Delta b_j - (C_{j m k l}^e \Delta \varepsilon_{kl}^*)_{,m} - \Delta r_j \right) (\mathbf{y}) d\mathbf{y} \quad (64)$$

where $g_{ij}(\mathbf{x}, \mathbf{y})$ is the fundamental solution of the differential operator $\mathcal{L}(\Delta \mathbf{u}) = \nabla \cdot (\mathbf{C}^e : \nabla^s \Delta \mathbf{u})$. With the consideration of large deformation, the Galerkin weak form of the homogeneous problem of Eq. (63) is transformed to the undeformed configuration Ω_X , and a Lagrangian kernel [6] is used to approximate the homogeneous solution following6:

$$\Delta u_i^0(\mathbf{X}) = \sum_{I=1}^{NP} \Psi_I(\mathbf{X}) \Delta d_{iI}^0 \quad (65)$$

where $\Psi_I(\mathbf{X})$ is the MLS/RK shape function using Lagrangian kernel. Note that the solution of homogeneous solution in Eq. (63) requires the particular solution in Eq. (64). Since the transformation of weak form of the homogeneous solution in Eq. (63) to the undeformed configuration requires the

particular solution to be evaluated in the unformed configuration, a mapping from \mathbf{x} to \mathbf{X} is needed. A stabilized conforming nodal integration (SCNI) that satisfies integration constraints in the Lagrangian Galerkin approximation of the homogeneous solution is employed in the domain integration of weak form in the undeformed configuration [8]. In SCNI, to meet integration constraints using nodal integration in Lagrangian Galerkin formulation, the displacement spatial gradient $\Delta u_{i,j} = \partial u_i / \partial x_j$ at a nodal point X_L in the undeformed configuration is smoothed as:

$$\Delta \tilde{u}_{i,j}^0(\mathbf{X}_L) = \Delta \tilde{F}_{ik}^0(\mathbf{X}_L) \tilde{F}_{kj}^{-1}(\mathbf{X}_L) \quad (66)$$

where

$$\Delta \tilde{F}_{ij}^0(\mathbf{X}_L) = \frac{1}{A_L^X} \int_{\Omega_L^X} \Delta F_{ij}^0 d\Gamma = \frac{1}{A_L^X} \int_{\Omega_L^X} \frac{\partial \Delta u_i^0}{\partial X_j} d\Gamma = \frac{1}{A_L^X} \int_{\Gamma_L^X} (\Delta u_i^0 N_j) d\Gamma \quad (67)$$

$$\tilde{F}_{ij}(\mathbf{X}_L) = \frac{1}{A_L^X} \int_{\Omega_L^X} F_{ij} d\Gamma = \frac{1}{A_L^X} \int_{\Omega_L^X} \frac{\partial u_i}{\partial X_j} d\Gamma + \delta_{ij} = \frac{1}{A_L^X} \int_{\Gamma_L^X} (u_i N_j) d\Gamma + \delta_{ij} \quad (68)$$

Here N_i is the surface normal in the undeformed configuration, Ω_L^X and Γ_L^X are the nodal representative domain and boundary of the Voronoi cell associated with node L in the undeformed configuration, respectively, and A_L^X is the area (volume) of Ω_L^X . The other details of Lagrangian meshfree method using SCNI for nonlinear problems can be found in [8]. Due to the absence of source term in the homogeneous problem, the Lagrangian meshfree formulation for solving the homogeneous solution can achieve much greater solution accuracy.

4.4 Numerical Example

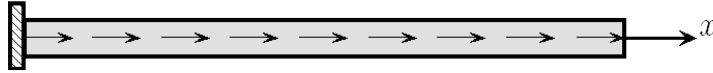


Fig. 7. One dimensional rod subjected body force

A one dimensional elasto-plastic bar subjected to a body force as shown in Fig. 7 is analyzed. In this example, the following isotropic hardening elasto-plasticity model is employed, where the yield function is expressed as:

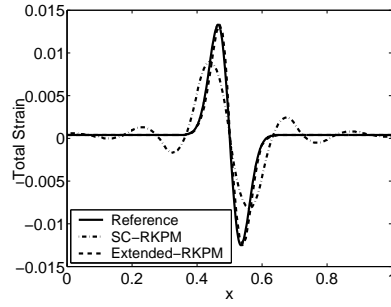


Fig. 8. Total strain comparison of elasto-plasticity problem

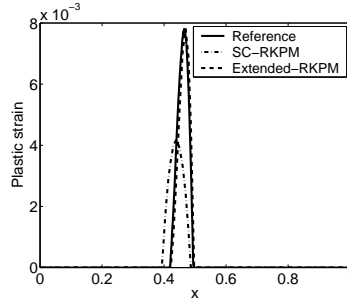


Fig. 9. Plastic strain comparison of elasto-plasticity problem

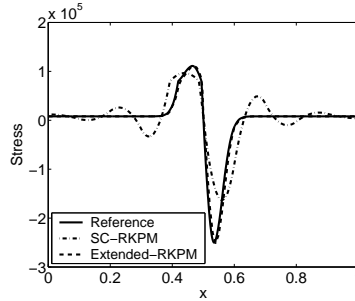


Fig. 10. Stress comparison of elasto-plasticity problem

$$f = |\sigma| - (\sigma_y + K\bar{\epsilon}^p) \quad (69)$$

Here, σ_y is the initial yield stress and K is hardening parameter. The material properties are: Young's modulus $E = 2.0 \times 10^7$, $K = 0.2E$ and $\sigma_y = 8.0 \times 10^4$. The body force function given in Eq. (7) is used, and the rod is fixed at the left end. Both SC-RKPM and the proposed Extended-RKPM are employed. The rod is discretized by only 8 nodes using both methods. For comparison purpose, a refined model with 51-node discretization is used to compute a reference solution. The numerical results for total strain, plastic

strain and stress distributions are shown in Figs. 8, 9, and 10, respectively. A much enhanced solution is observed in the proposed new approach.

5 Conclusions

An extended meshfree method for elastic and inelastic media has been presented. In this approach, the total solution has been expressed by a combination of particular and homogeneous solutions. The particular solution is any analytical (or numerical) expression satisfying the governing differential equation containing the source term but not necessarily the boundary conditions. Thus, the problem is reduced to a homogeneous equation where the original boundary conditions are modified by the particular solution. In this paper, a general method has been presented for constructing the particular solution. The homogeneous solution has been solved numerically using Galerkin approximation. By employing moving least-square reproducing kernel (MLS/RK) approximation with linear completeness, as well as a stabilized conforming nodal integration (SCNI) for domain integration of the weak form, a linear exactness in solid continuum and a bending exactness in plate bending can be achieved in the homogeneous counterpart of these problems. Compared to the conventional Galerkin meshfree method, this new approach significantly reduces the constant in the error norms, and examples have been demonstrated in Poisson, elasticity, and Mindlin-Reissner plate problems.

The proposed method for differential equations with nonlinear differential operators has also been presented. It has been shown that if the differential operator is self-adjoint, a homogeneous problem can be obtained with standard integration by parts procedures. A Lagrangian MLS/RK approximation and the corresponding SCNI for Lagrangian weak form of large deformation problems have also been discussed. Using elasto-plasticity as a model problem, a simplified approach to obtain particular solution and to construct homogeneous problem has been presented. In this approach, the nonlinearity resides in the source term, and the differential operator takes the form of linear elasticity. Thus the fundamental solution is identical to that of linear elasticity, and the particular solution is obtained by integration of fundamental solution and the nonlinear source term at every incremental step in nonlinear calculation. The corresponding homogeneous problem has been constructed with boundary conditions corrected by the particular solution in every incremental step, and it has been solved using MLS/RK approximation with SCNI domain integration of the incremental weak form. The numerical results demonstrate a substantially higher solution accuracy in extended meshfree method compared to that of the conventional Galerkin meshfree method.

6 Appendix

The parameters and matrices used Table 1 are defined as follows:

$$P_1 = \frac{Et^3}{24(1+\nu)}, \quad P_2 = \frac{Et^3}{24(1-\nu)}, \quad Q = \frac{5Et}{12(1+\nu)}, \quad D = \frac{Et^3}{12(1-\nu^2)} \quad (70)$$

$$[\hat{\nabla}] = \begin{bmatrix} \frac{\partial}{\partial x_1} & 0 & 0 \\ 0 & \frac{\partial}{\partial x_2} & 0 \\ 0 & 0 & \frac{\partial}{\partial x_3} \\ \frac{\partial}{\partial x_2} & \frac{\partial}{\partial x_1} & 0 \\ \frac{\partial}{\partial x_3} & 0 & \frac{\partial}{\partial x_1} \\ 0 & \frac{\partial}{\partial x_3} & \frac{\partial}{\partial x_2} \end{bmatrix}, \quad [\bar{\nabla}] = \begin{bmatrix} \frac{\partial}{\partial x_1} & 0 \\ 0 & \frac{\partial}{\partial x_2} \\ \frac{\partial}{\partial x_2} & \frac{\partial}{\partial x_1} \end{bmatrix}, \quad \nabla = \left\{ \begin{array}{c} \frac{\partial}{\partial x_1} \\ \frac{\partial}{\partial x_2} \end{array} \right\} \quad (71)$$

$$[\mathbf{N}] = \begin{bmatrix} -1 & 0 & \frac{\partial}{\partial x_1} \\ 0 & -1 & \frac{\partial}{\partial x_2} \end{bmatrix}, \quad [\mathbf{G}] = [-\mathbf{D}^b [\bar{\nabla}] \quad \{\mathbf{0}\}] \quad (72)$$

$$[\mathbf{D}^b] = \frac{Et^3}{12(1-\nu^2)} \begin{bmatrix} 1 & \nu & 0 \\ \nu & 1 & 0 \\ 0 & 0 & \frac{(1-\nu)}{2} \end{bmatrix}, \quad [\mathbf{D}^s] = \frac{5}{6}t\mu \begin{bmatrix} 1 & 0 \\ 0 & 1 \end{bmatrix} \quad (73)$$

Acknowledgement: The support of this work by NSF grant CMS-0296112 to UCLA is greatly acknowledged.

References

- [1] I. Babuska, U. Banerjee and J.E. Osborn: Survey of meshless and generalized finite element methods: a unified approach. *Acta Numerica*, 1–125(2003).
- [2] I. Babuska and J. M. Melenk: The partition of unity finite element method. *Int. J. Numer. Meth. Eng.*, **40**,727–758(1997).
- [3] T. Belytschko, N. Moes, S. Usui and C. Parimi: Arbitrary discontinuities in finite elements. *Int. J. Numer. Meth. Eng.*, **50**, 993–1013(2001).
- [4] T. Belytschko, Y.Y. Lu and L. Gu: Element-free Galerkin methods. *Int. J. Numer. Meth. Eng.*, **37**,229–256(1994).
- [5] C.A. Brebbia, J. Dominguez: Boundary elements: an introductory course. *Computational mechanics publications*, McGraw-Hill book company (1989).
- [6] J.S. Chen, C. Pan, C.T. Wu and W.K. Liu: Reproducing kernel particle methods for large deformation analysis of nonlinear structures. *Comput Meth. Appl. Mech. Engng.*, **139**, 195–227(1996).
- [7] J.S. Chen, C.T. Wu, S. Yoon, and Y. You: A stabilized conforming nodal integration for Galerkin meshfree methods. *Int. J. Numer. Meth. Eng.*, **50**, 435–466(2001).

- [8] J.S. Chen, C.T. Wu and S. Yoon: Nonlinear version of stabilized conforming nodal integration for Galerkin meshfree methods. *Int. J. Numer. Meth. Eng.*, **53**,2587–2615(2002).
- [9] J.S. Chen, D. Wang and S.B. Dong: An extended meshfree method for boundary value problems. *Comput. Meth. Appl. Mech. Engng.*, **193**, 1085–1103(2004).
- [10] J. Dolbow, N. Moes and T. Belytschko: Discontinuous enrichment in finite elements with a partition of unity method. *Finite Elements Anal. Design*,**36**,235–260(2000).
- [11] C.A.M. Duarte and J.T. Oden: A h-p adaptive method using clouds. *Comput.Meth. Appl. Mech. Engng.*, **139**,237–262(1996).
- [12] C. A. M. Duarte, I. Babuska, and J. T. Oden: Generalized finite element method for three dimensional structural problems. *Computer and Structures*, **77**, 219–232(2000).
- [13] A. Huerta and S. Fernández-Méndez: Enrichment and coupling of the finite element and meshless methods. *Int. J. Numer. Meth. Eng.*, **48**, 1615–1636(2000).
- [14] Y. Krongauz and T. Belytschko: EFG Approximation with discontinuous derivatives, *Int. J. Numer. Meth. Eng.*, **41**, 1215–1233(1998).
- [15] Y. Krongauz and T. Belytschko: Enforcement of essential boundary conditions in meshless approximations using finite elements. *Comput. Meth. Appl. Mech. Engng.*, **131**, 133–145(1996).
- [16] S. Li and W. K. Liu: Reproducing kernel hierarchical partition of unity part I: formulation and theory. *Int. J. Numer. Meth., Eng.*, **45**,251–288 (1999).
- [17] W.K. Liu, R.A. Uras and Y. Chen: Enrichment of the finite element method with the reproducing kernel particle method. *Journal of Applied Mechanics*, **64**, 861–870(1997).
- [18] W.K. Liu, S. Jun, Y.F. Zhang: Reproducing kernel particle methods. *Int. J. Numer. Meth. Fluids*, **20** 1081–1106(1995).
- [19] J.M. Melenk and I. Babuska: The partition of unity finite element method: basic theory and applications. *Comput. Meth. Appl. Mech. Engng.*,**139**, 289–314(1996).
- [20] T. Strouboulis, I. Babuska, and K. Copps: The design and analysis of the generalized finite element method, *Comput. Meth. Appl. Mech. Engng.*,**181**, 43–69(2001).
- [21] T. Strouboulis, K. Copps, and I. Babuska: The generalized finite element method. *Comput. Meth. Appl. Mech. Engng.*, **190**, 4081–4193(2001).
- [22] G.J. Wagner and W.K. Liu: Hierarchical enrichment for bridging scales and meshfree boundary conditions. *Int. J. Numer. Meth. Eng.*, **50**, 507–524(2001).
- [23] D. Wang and J.S. Chen: Locking-free stabilized conforming nodal integration for meshfree Mindlin-Reissner plate formulation. *Comput. Meth. Appl. Mech. Engng.*, **193**, 1065–1083(2004).
- [24] D. Wang, J.S. Chen and L. Sun: Homogenization of magnetostrictive particle-filled elastomers using an interface-enriched reproducing kernel particle method. *Finite Element Anal. Design*, **39**, 765–782(2003).
- [25] Y. Wang: *Boundary elements in engineering*. China Hydraulic and Hydroelectric Press, Beijing (1995).